

Efficient Fluorescent Recognition of Carboxylates in Aqueous Media Using Facilely Electrosynthesized Poly(9-Amino fluorene)

Ge Zhang · Yangping Wen · Yuzhen Li · Jingkun Xu ·
Chaoqun Guo · Baoyang Lu · Danhua Zhu

Received: 12 January 2013 / Accepted: 9 May 2013 / Published online: 29 May 2013
© Springer Science+Business Media New York 2013

Abstract A variety of carboxylates were recognized using poly(9-amino fluorene) (P9AF) in the HEPES buffer (pH 7.4), and a proposed possible mechanism was proposed as following. The intermolecular hydrogen bonding interactions resulted in electron transfer between P9AF and carboxylates. P9AF was facilely electrosynthesized in boron trifluoride diethyl etherate and could be used as an efficient fluorescent sensing material for the detection of AcO^- . On binding to AcO^- , fluorescence quenching of P9AF was demonstrated by a maximum 80 % reduction in the fluorescence intensity, while no obvious fluorescence change could be observed in the presence of some other common anions. Some different carboxylates could be recognized at different levels by P9AF. Substituent groups in carboxylates could affect the intermolecular interaction between carboxylates and P9AF. These could be explained by a possible mechanism that hydrogen bonding was the main way of intermolecular interactions between P9AF and carboxylates,

which was further confirmed by absorption spectra monitoring and density functional calculations. The significant advantage of this strategy is that it does not require a prequenching procedure and the polymer can be used directly for analyte detection.

Keywords Carboxylates · Fluorescence quenching · Conjugated polymer · Electrochemical synthesis · Density functional calculation

Introduction

Anions play a major role in many biological processes and in biological structures, such as amino acids, neurotransmitters, organic acids, enzyme substrates, co-factors, and nucleic acids. They are also important components in a variety of industries, such as in the production of fertilisers, in food additives, and in the water supply [1, 2]. Thus, the determination of anions in biological and industrial processes has attracted increasing interests. With this consideration, fluorescence-based sensors have been of particular interest because of their high sensitivity, versatility, and fairly good selectivity. The most desirable property of a fluorescence anion sensor is the ability to respond to applied perturbation in a highly selective and sensitive manner by dramatic change in emission color and/or intensity. Among different kinds of anions, carboxylates are important target species in molecular recognition as they serve important functions in biological systems. For this purpose, many fluorescent sensors for carboxylate anions have been developed on the basis of a variety of signaling mechanisms such as competitive binding, photo-induced electron transfer, metal-to-ligand charge transfer, excimer/exiplex, and intramolecular charge transfer [3–7].

Ge Zhang and Yangping Wen contributed equally to this work.

Electronic supplementary material The online version of this article (doi:10.1007/s10895-013-1234-6) contains supplementary material, which is available to authorized users.

G. Zhang · Y. Wen · J. Xu (✉) · C. Guo · B. Lu · D. Zhu
Jiangxi Key Laboratory of Organic Chemistry, Jiangxi Science and
Technology Normal University, Nanchang 330013, China
e-mail: xujingkun@tsinghua.org.cn

Y. Wen
Key Laboratory of Crop Physiology, Ecology and Genetic
Breeding, Ministry of Education, Jiangxi Agricultural University,
Nanchang 330045, China

Y. Li
Department of Chemistry, Shanghai Key Laboratory of Molecular
Catalysts and Innovative Materials, Fudan University, Shanghai
200433, China

Recently, fluorescent conjugated polymer molecular wires have been widely explored as highly sensitive chemosensors because they can offer a myriad of opportunities for coupling analyte-receptor interactions, as well as nonspecific interactions, into an observed response. In comparison with the conventional small molecular-based fluorescent chemosensors, conjugated polymer-based fluorescent chemosensors show enhanced sensitivity due to intrinsic signal amplification, which coordinate the action of a large number of optically active absorbing units with delocalized electronic structures [8, 9]. Important properties of conjugated polymers (CPs) such as charge transport, conductivity, emission intensity, and exciton migration, are easily perturbed by external agents, leading to substantial changes in measurable signals [8–11]. Fluorescent chemosensors based on polymers have several important advantages, such as their simplicity of use, signal amplification, easy fabrication into devices, and combination of different outputs. Swager et al. firstly establish this concept through a supposed theory that the receptors are interconnecting as a molecular wire, in which the energy migration may occur along the polymer backbone upon the excitations due to the conductivity of the backbone. Consequently, the polyreceptor system produces a response larger than that afforded by a small interaction in an analogous small monoreceptor system [9–11]. In CP-based sensors, only fractional binding of analyte can cause an amplified signal due to delocalization of exciton along the conjugated chain. Poly(p-phenylene)s [12], poly(p-phenylene ethynylene)s [13], poly(p-phenylene vinylene)s [14], polythiophenes [15], and polyfluorenes [16] with receptor groups, e.g., crown ethers [17] pyridine derivatives [18] and ionic groups [19] in the side chain or main chain have been successfully used for sensing ions and biological species.

It should be noted that most fluorescent CPs with rigid structures can only work in the organic solvents which prevent their potential application in medical and biological system. Recent studies show that incorporation of anionic or cationic functionalities into CPs yield new materials possessing the beneficial properties of CPs with aqueous solubility. Plenty of new water-soluble CPs have been designed and synthesized by many groups all over the world, and advances in biological and chemical applications of these water-soluble CPs have been made [20–22]. Shinkai and coworkers reported a water-soluble poly(thiophene)-based sensor for adenosine triphosphate (ATP) [20]. Heeger et al. reported that cationic conjugated polyfluorene derivative was quenched with exceptional efficiency by gold nanoparticles in water [21]. Therefore, water-soluble CPs provide a unique platform for the construction of chemical and biological sensors. The commonly employed reactions for the synthesis of water-soluble CPs are known as palladium-catalyzed coupling reactions (Suzuki, Heck, and Sonogashira), Wessling reaction, topopolymerization reaction, and FeCl_3 oxidative polymerization [22]. Although most of polymers are synthesized by these chemical methods, the

electrochemical method has significant advantages of rapid analyses, accuracy, precision, and requiring small amounts of material [23, 24]. Shi group successfully synthesized a series of water-soluble polypyrene derivatives via electrochemical polymerization and employed these CPs to detect various analytes [25–27].

Polyfluorene (PF) and its derivatives have been considered promising candidates as blue-light-emitting materials because of their highly efficient photoluminescence and electroluminescence, thermal and oxidative stability, and emission of polarized blue light [28–30]. Therefore, during the past decades remarkable advances have been made in the production of PF derivations which are used to sense anions [31, 32]. Liu et al. prepared two cationic poly(fluorene-alt-benzothiadiazole) polymers and tested their sensing ability toward heparin and hyaluronic acid [32]. Our group has been studying the electrochemical synthesis, characterization, and applications of CPs, including PF, poly(9-aminofluorene) (P9AF), poly(9-hydroxyfluorene), poly(9-fluorenicarboxylic acid), and poly(9-hydroxyfluorene-9-carboxylic acid) [33–35]. Substitution of an amino group on the PF backbone gives P9AF special good solubility in water. The cost-effective, water-soluble, and easily electrosynthesized P9AF has been successfully employed to sense Fe(III) and inorganic phosphates (pH 7.0) in living cells with satisfying results [36].

Inspiring results prompted us to take further this motif in the construction of new anions sensor. In this study, P9AF was electrosynthesized and developed as a fluorescent chemosensor for recognition of AcO^- anions in the 10 mM HEPES buffer (pH 7.4). Furthermore, P9AF was used to recognize a variety of carboxylates with different fluorescence quenching efficiencies. Finally, a possible mechanism was

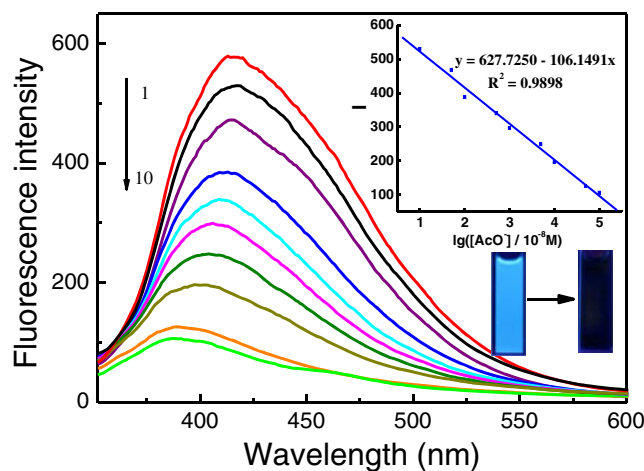


Fig. 1 The fluorescence emission spectra of P9AF (5.0×10^{-7} M in repeat units) in the HEPES buffer (pH 7.4) with successive addition of AcO^- : (1) blank; (2) 9.99×10^{-8} M; (3) 4.99×10^{-7} M; (4) 9.97×10^{-7} M; (5) 4.98×10^{-6} M; (6) 9.95×10^{-6} M; (7) 4.97×10^{-5} M; (8) 9.93×10^{-5} M; (9) 4.96×10^{-4} M; (10) 9.91×10^{-4} M. Inset: Relationship between the relative fluorescence of P9AF and AcO^- concentration. Excitation was at 342 nm

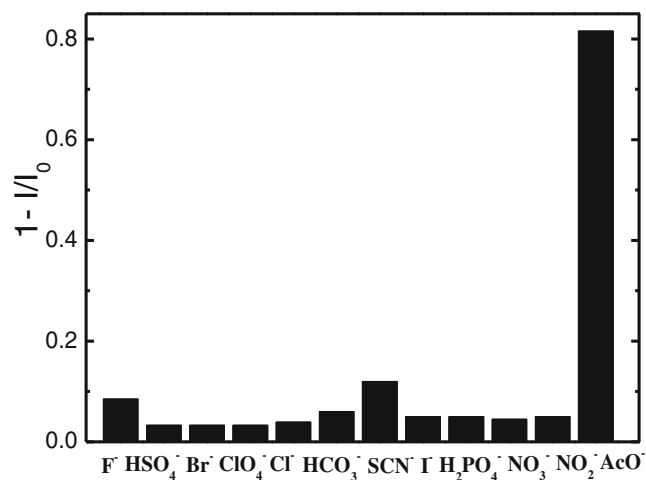


Fig. 2 Fluorescence quenching efficiencies of P9AF (5.0×10^{-7} M in repeat units) in the presence of various anions (each 1 mM) in the HEPES buffer (pH 7.4). I_0 corresponds to the fluorescence emission of solution without AcO^- and I to the fluorescence emission of solution with AcO^-

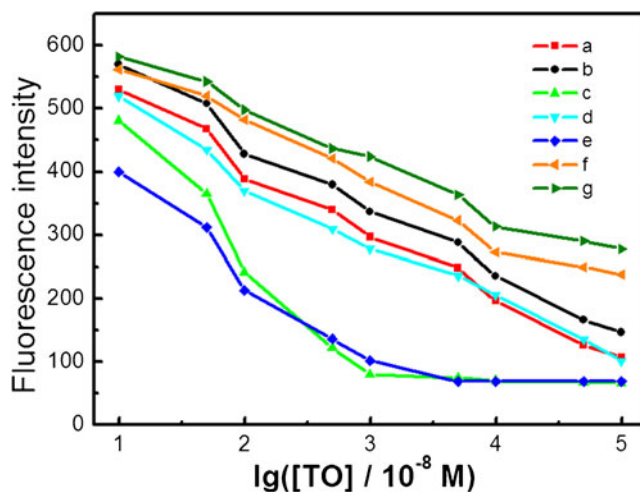


Fig. 3 Plots of the fluorescence maximum intensity of P9AF (5.0×10^{-7} M in repeat units) versus test objects (TO) concentration. *a* sodium acetate, *b* sodium glycinate, *c* sodium oxalate, *d* sodium glutamate, *e* sodium citrate, *f* sodium benzoate, *g* sodium salicylate

discussed via absorption spectra monitoring and density functional calculations.

Experimental

Reagents and Materials

9AF (99 %; Acros Organics, Belgium) was used as received. Boron trifluoride diethyl etherate (BFEE) (Beijing Changyang Chemical Plant, China) was distilled and stored at -20°C before use. Twice-distilled water was used throughout all experiments. HEPES was obtained from Aldrich. Unless otherwise stated, all fluorescent tests were performed in the 10 mM HEPES buffer (pH 7.4). Sodium acetate, sodium glycinate, sodium oxalate, sodium glutamate, sodium citrate, sodium benzoate, sodium salicylate, formic acid, acetic acid, propionic acid, isobutyric acid, pivalic acid, benzoic acid, 9-fluorencarboxylic acid, oxalic

acid, glutamic acid, tricarballic acid, citric acid, trifluoroacetic acid, trichloroacetic acid, tribromoacetic acid, acrylic acid, methyl acrylate, butyl acrylate, and 2-ethylhexyl acrylate were obtained from commercial suppliers. Note: methyl acrylate, butyl acrylate, and 2-ethylhexyl acrylate were dissolved in ethanol and others were dissolved in water.

Apparatus

Electrochemical polymerization and tests were performed in a one-compartment cell using a model 263A potentiostat-galvanostat (EG & G Princeton Applied Research) under computer control. Absorption spectra were measured using an Agilent 8453 UV/VIS spectrophotometer. All fluorescence experiments were carried out using a Hitachi F-4500 spectrophotometer with excitation slit set at 5 nm and emission slit at 5 nm. The pH values were tested by a pen-like pH meter (CT-6022, Shanghai Rentong Meter CO., Ltd). Gel permeation

Table 1 Parameters and performance of the different AcO^- fluorescent sensor in previous reports

| Fluorophore | Solvent | Concentration of fluorophore (M) | Working of concentration range (M) | Limit of detection (M) | References |
|----------------------------|-----------------------------------------------------------------------|----------------------------------|------------------------------------|------------------------|------------|
| Anthracene derivative 2 | DMSO | 1.0×10^{-5} | $(0-3.2) \times 10^{-2}$ | ND | [39] |
| Anthracene derivative 1 | DMSO | 2.0×10^{-6} | $(0-8.0) \times 10^{-4}$ | ND | [40] |
| 3-hydroxyl-2-naphthanilide | CH_3CN | 1.0×10^{-5} | $(0-2.0) \times 10^{-5}$ | ND | [41] |
| Thiourea derivative | CH_3CN | 8.0×10^{-6} | $(0-1.1) \times 10^{-5}$ | ND | [42] |
| Naphthalene derivative 1 | CH_3CN | 1.0×10^{-5} | $(0-2.0) \times 10^{-3}$ | ND | [43] |
| Uranyl salophen L | $\text{CH}_3\text{CN}/\text{H}_2\text{O} = 9/1$ (v/v) | 5.0×10^{-6} | $(1.6-250) \times 10^{-7}$ | 2.5×10^{-8} | [44] |
| 3HF-Al(III) complex | CH_3OH | ND | $(0-6.8) \times 10^{-5}$ | ND | [45] |
| Anthracene derivative 1 | $\text{DMSO}/\text{H}_2\text{O} = (95:5, \text{v/v})$ HEPES buffer | 4.0×10^{-5} | $(0-2.2) \times 10^{-4}$ | ND | [46] |
| P9AF | HEPES buffer (pH = 7.4) | 5.0×10^{-7} | $(0.999-9910) \times 10^{-7}$ | 4.45×10^{-9} | This work |

chromatography (GPC) measurements of the P9AF were performed in tetrahydrofuran with a Waters Breeze GPC system. Quantum chemical calculations were performed to determine the interaction between carboxylates and P9AF. Geometry optimization, relative energy and harmonic vibrational frequency analysis were performed with the most popular hybrid-GGA B3LYP density functional theory (DFT) method with the 6-31+G(d) basis set for H, C, O, N and F atoms using the Gaussian 09 program [37].

Syntheses

P9AF was electrosynthesized in BFEE containing 0.02 mol L^{-1} 9AF. The amount of the resulting polymers deposited on the surface of the working electrode was controlled by the integrated current passed through the cell. Polymer films were rinsed

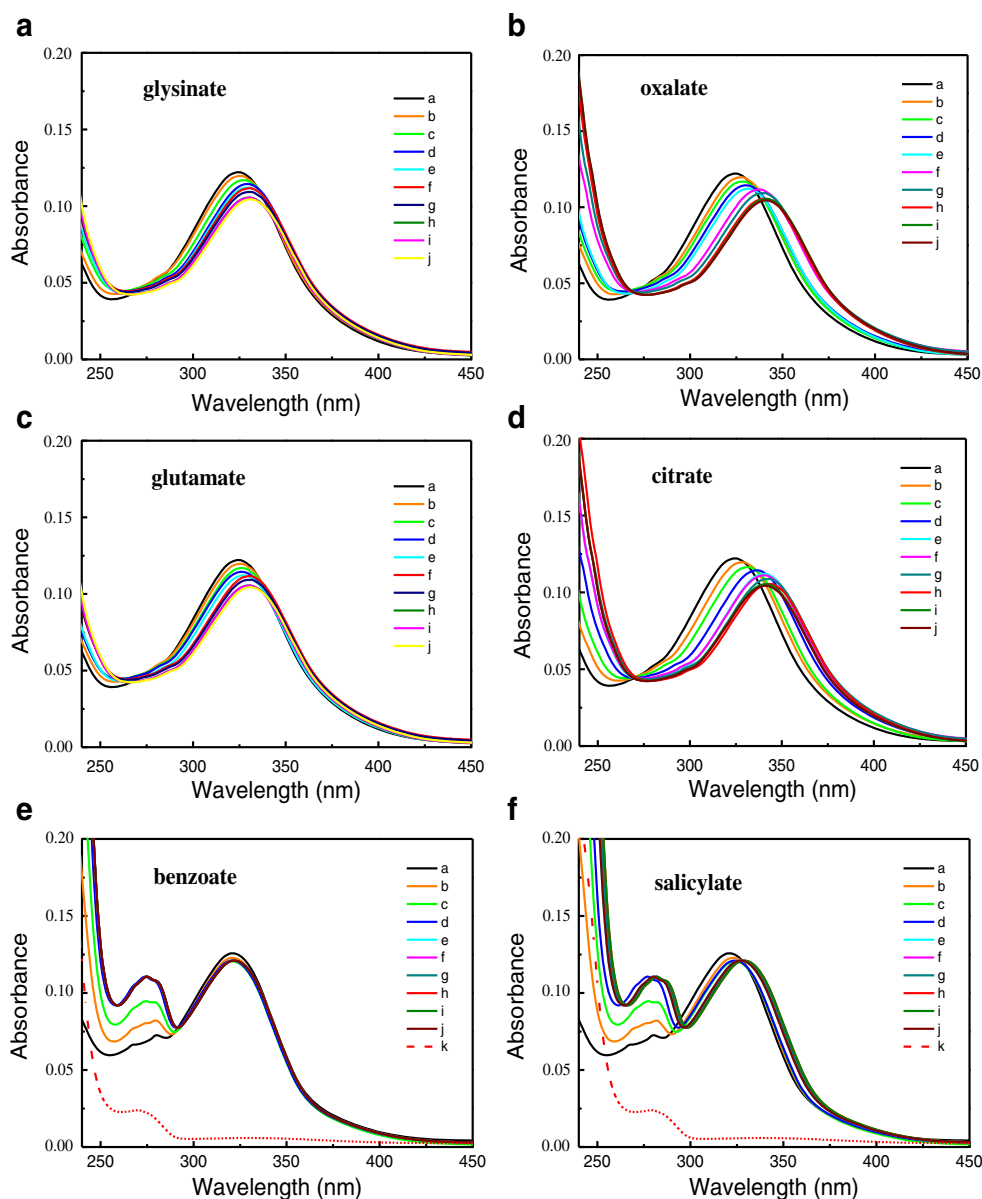
with diethyl ether to remove the electrolyte, oligomers, and monomer. The as-obtained P9AF films were in the doped state, dark metallic in color, and were soluble in water. The molecular weight of polymers was measured by GPC ($M_n=6021$, $M_w=6573$). For spectral analyses, Polymers were dedoped with 25 % ammonia for 3 days. The dedoped films were then dried under vacuum at $60 \text{ }^\circ\text{C}$ for 24 h.

Results and Discussion

Electrochemical Polymerization of P9AF

P9AF was facilely obtained by the direct electropolymerization of commercially available monomer 9AF in pure BFEE (Fig. S1). The electrochemistry, thermal stability, and structural

Fig. 4 UV-vis titration of P9AF in the HEPES buffer (pH 7.4) with increasing concentration of carboxylate anions: *a* blank; *b* $9.99 \times 10^{-8} \text{ M}$; *c* $4.99 \times 10^{-7} \text{ M}$; *d* $9.97 \times 10^{-7} \text{ M}$; *e* $4.98 \times 10^{-6} \text{ M}$; *f* $9.95 \times 10^{-6} \text{ M}$; *g* $4.97 \times 10^{-5} \text{ M}$; *h* $9.93 \times 10^{-5} \text{ M}$; *i* $4.96 \times 10^{-4} \text{ M}$; *j* $9.91 \times 10^{-4} \text{ M}$



characterization of water-soluble P9AF were studied in detail in our previous work, and the fluorescence spectra suggested that water-soluble P9AF was a good blue-light emitter [33]. Then, P9AF was employed to sense cations and had highly selective and sensitive to Fe^{3+} , and inorganic phosphates could recover this P9AF- Fe^{3+} quenching system in the HEPES buffer (pH 7.0). This technology has been applied in cell images with satisfying results [36]. Inspired by these aspects, we studied the sensing of anions by P9AF in the following study.

Anion Binding Studies of P9AF

It is well known that fluorescent emission spectroscopy is more sensitive toward small changes that affect the electronic properties of molecular receptors. Herein, titration of P9AF with AcO^- (as sodium salt) was monitored by a photoluminescent technique at physiological pH value (pH 7.4) in the 10 mM HEPES buffer. Figure 1 displayed the fluorescence spectra upon titration of P9AF (5.0×10^{-7} M in repeat units) with AcO^- . Upon addition of AcO^- , emission intensity immediately decreased with an emission blue shift up to 25 nm which could be observed with the ‘naked-eye’. In addition, the relationship between fluorescence intensity (I) and the AcO^- concentration $[\text{AcO}^-]$ of the fabricated sensor containing various $[\text{AcO}^-]$ was shown in Fig. 1. Obviously, I gradually decreased with increasing $[\text{AcO}^-]$, revealing that this method was suitable for detecting the unknown content of AcO^- . I vs. $\lg[\text{AcO}^-]$ depicted the relationship between I and the common logarithm of $[\text{AcO}^-]$ ($\lg[\text{AcO}^-]$). The I vs. $\lg[\text{AcO}^-]$ graph in Fig. 1 inset revealed that there was a good linearity of the common I vs. $\lg[\text{AcO}^-]$ from 99.9 nM to 0.991 mM ($y = -106.1491x + 627.7250$ ($R^2 = 0.9898$)). The limit of detection (LOD) was calculated using the following equations [38]:

$$\text{LOD} = 3s/m$$

where s is the standard deviation of the lowest concentration of the linearity range and m is the slope of linear equation in Fig. 1 inset. The detection limit was found to be 4.45 nM. These results indicated that water-soluble P9AF could be used as a fluorescent sensor for AcO^- . To validate the specificity of P9AF toward anionic guests, the changes in the fluorescence intensity of P9AF upon addition of some anions such as F^- , Cl^- , Br^- , I^- , ClO_4^- , HSO_4^- , NO_3^- , NO_2^- , HCO_3^- , SCN^- , and H_2PO_4^- were studied. Figure 2 revealed fluorescence emission response profiles of P9AF up addition different anions with the concentration of 1 mM. Almost no emission quenching was observed upon addition of Cl^- , Br^- , I^- , HSO_4^- , NO_3^- , NO_2^- , H_2PO_4^- and ClO_4^- . P9AF was slightly active to F^- , SCN^- , and HCO_3^- , but had the highest sensitivity to AcO^- .

Of the analytes studied here, these results indicated that the quenching of fluorescence was much more effective in the presence of AcO^- than with the use of other anions and that

the detection limit could be extended to the order of 10^{-9} M. To elucidate the interaction behind the remarkable fluorescence quenching observed for P9AF in the presence of AcO^- , the UV-vis spectra of P9AF were studied as well in the presence AcO^- . As shown in Fig. S2, the absorption maximum of P9AF was exhibited at 325 nm, which red shifted upon adding AcO^- anions. This is presumably due to perturbation of the HOMO energy levels of the sensors mainly localized on the fluorene moieties. The presence of the anion raises the energy level of the HOMO causing a red shift in the absorption. At $[\text{AcO}^-] = 0.496$ mM, the absorption spectra of P9AF was gradually levelled off, indicating the analyte-receptor saturation. The changes in the absorption spectra of

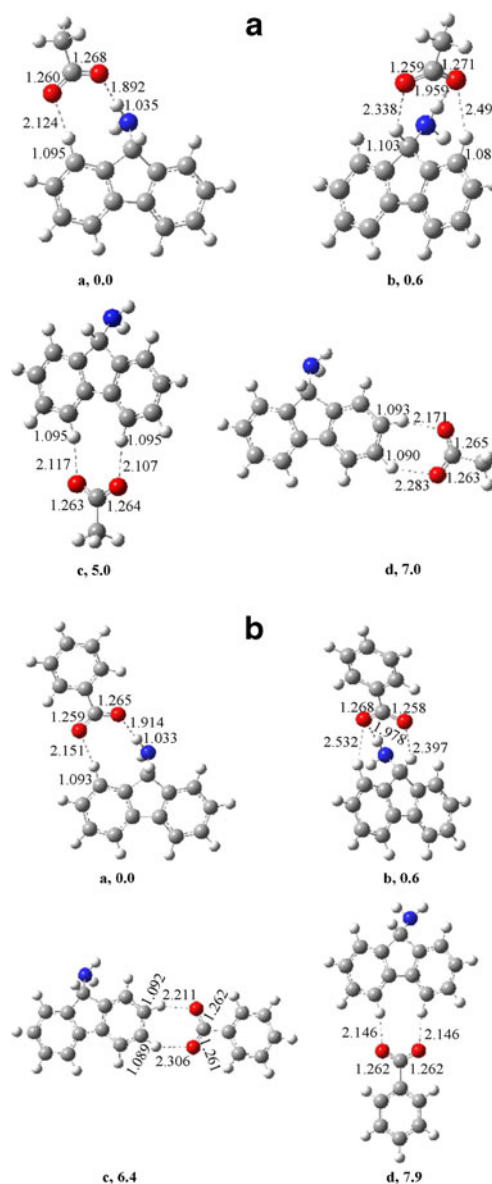
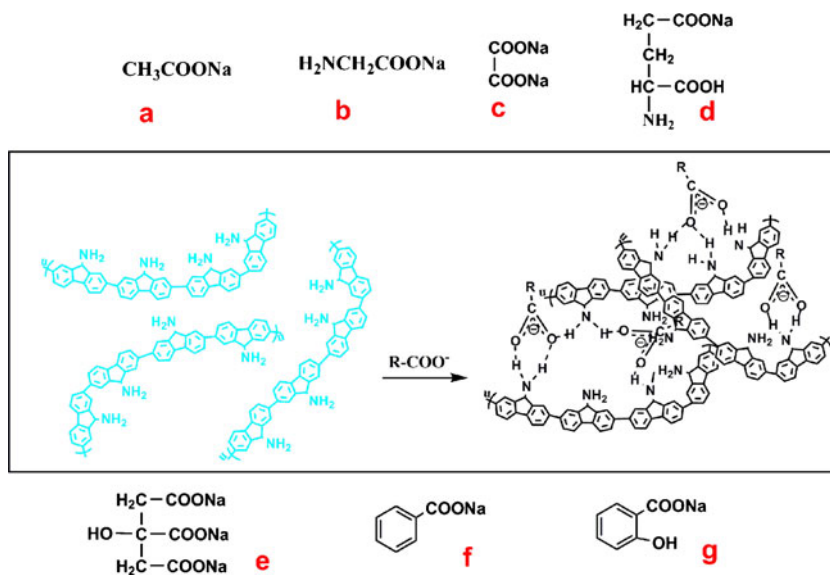


Fig. 5 Optimized structures for complexes formed from P9AF and carboxylate anions (**a** AcO^- , **b** benzoate) by B3LYP/6-31+G(d) method. The relative energies are given in kcal/mol

Scheme 1 Schematic illustration of the intermolecular hydrogen-binding interaction between P9AF and carboxylate anions



P9AF upon addition F^- , Cl^- , Br^- , I^- , ClO_4^- , HSO_4^- , HCO_3^- , SCN^- , NO_3^- , NO_2^- , and $H_2PO_4^-$ were studied. It was found that absorption bands of P9AF did not show any significant shift upon addition of Cl^- , Br^- , I^- , ClO_4^- , HCO_3^- , SCN^- , NO_3^- , NO_2^- , and HSO_4^- . After addition of an equimolar amount of F^- and $H_2PO_4^-$, the absorption bands of P9AF decreased without any shift (Fig. S3).

In previous reports, AcO^- can be detected using colorimetric sensors, fluorescent sensors, and electrochemical sensors etc [3–7]. As can be listed in Table 1, the as-fabricated sensor

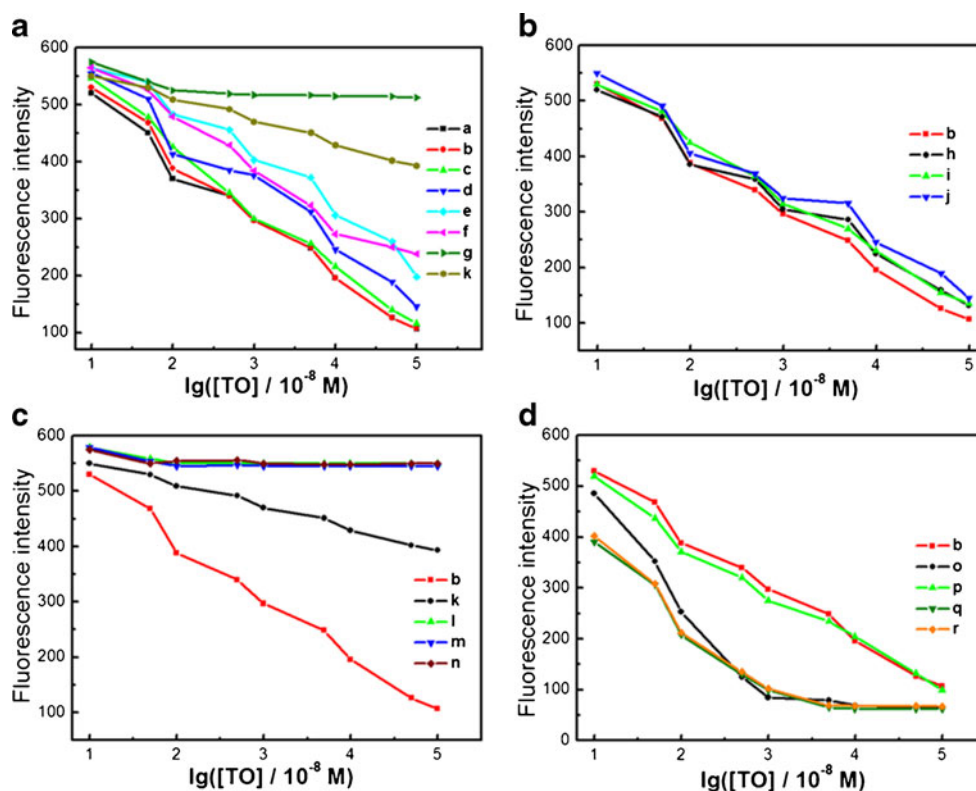
exhibits better performance in terms of the sensitivity, linear range, detection limits, and selectivity [39–46]. Moreover, the sensing material exhibits good water solubility, facile preparation, and low cost.

Recognition of Carboxylate Anions Using P9AF

The analytical determination of AcO^- with P9AF indicated that P9AF could be applied as a satisfactory AcO^- sensor in the HEPES buffer (pH 7.4). AcO^- possesses a $-COO^-$ compared

Fig. 6 Plots of the fluorescence maximum intensity of P9AF (5.0×10^{-7} M in repeat units) versus TO concentration.

a formic acid, *b* acetic acid, *c* propionic acid, *d* isobutyric acid, *e* pivalic acid, *f* benzoic acid, *g* 9-fluorenicarboxylic acid, *h* trifluoroacetic acid, *i* trichloroacetic acid, *j* tribromoacetic acid, *k* acrylic acid, *l* methyl acrylate, *m* butyl acrylate, *n* 2-ethylhexyl acrylate, *o* oxalic acid, *p* glutamic acid, *q* tricarballylic acid, *r* citric acid

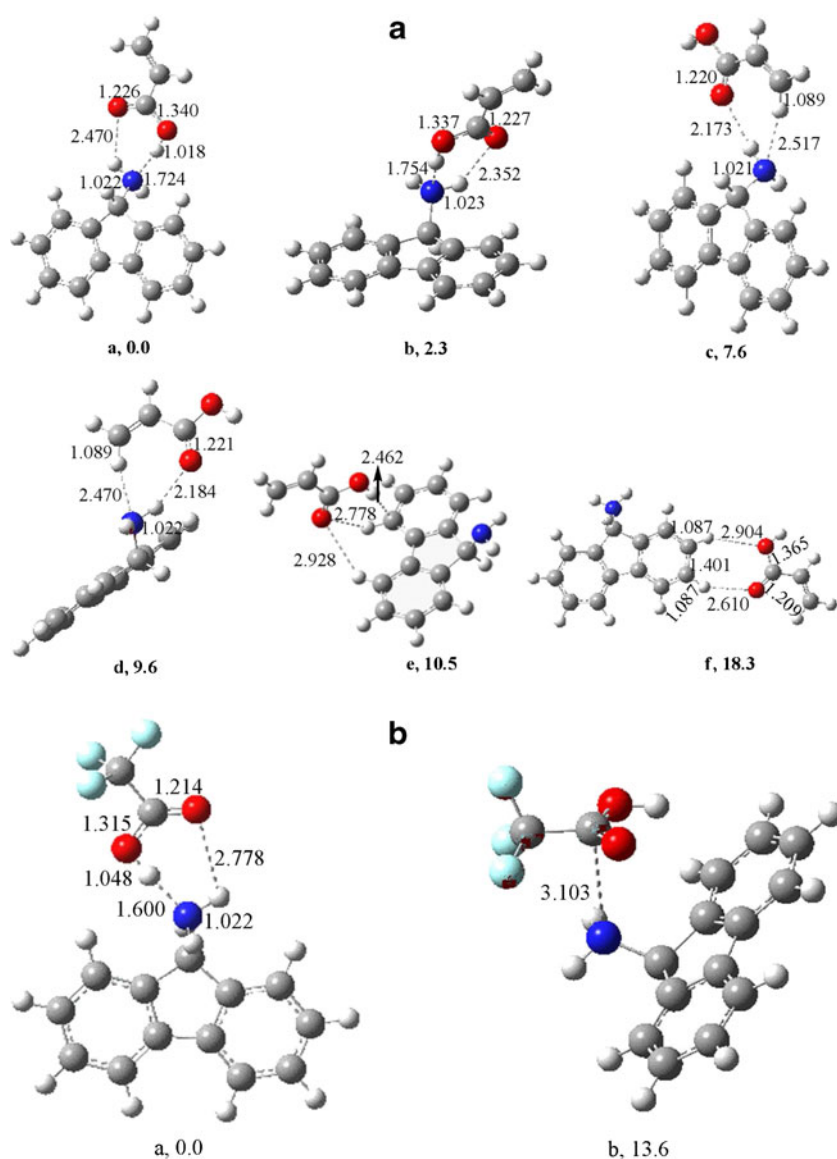


with other detected anions, which may have an interaction with P9AF. Intrigued by this fact, we detected some carboxylate anions using P9AF in the same conditions. As shown in Fig. 3, the fluorescence quenching efficiencies of P9AF with carboxylate anions were in decreasing order: citrate (e) > oxalate (c) > glutamate (d) > acetate (a) > glycinate (b) > benzoate (f) > salicylate (g). It showed that these carboxylate anions could be sensed in the HEPES buffer. The fluorescence quenching efficiencies slightly increased with the increasing number of COO^- (from a, c, e) in comparison to acetate (a), but decreased with introduction of substituent groups such as amino group (-NH_2), hydroxyl group (-OH), and phenyl group. These phenomena showed that substituent groups affect the interaction between COO^- and P9AF. In view of this fact, we studied the changes in the absorption spectra of P9AF upon addition of aforementioned carboxylate anions (Fig. 4). Absorption spectra of P9AF showed a redshift upon gradual addition of oxalate and

citrate, which were similar to AcO^- . But there was a smaller redshift upon addition of glycinate and glutamate, which was due to the effect of the substituent group (-NH_2). After adding benzoate and salicylate, the absorption spectra of P9AF increased at 275 nm, but only a little change at 325 nm. From Fig. 4e and f, the absorbance of benzoate and salicylate were approximately at 280 nm, e.g., the interaction between benzoate or salicylate and P9AF was weaker than AcO^- , which was due to the influence of phenyl group and -OH .

Absorption spectra monitoring revealed that there were interactions between P9AF and carboxylate anions. To determine the interaction between carboxylate anions and P9AF, we calculated the structures of complexes formed from P9AF with carboxylate ions and their relative energies by B3LYP/6-31+G(d) method, considering the three modes of intermolecular interactions: the hydrogen bonding interaction, the interaction between carboxyl carbon atoms and amino nitrogen atoms,

Fig. 7 Optimized structures for complexes formed from P9AF and carboxylates (**a** acrylic acid, **b** trifluoroacetic acid) by B3LYP/6-31+G(d) method. The relative energies are given in kcal/mol



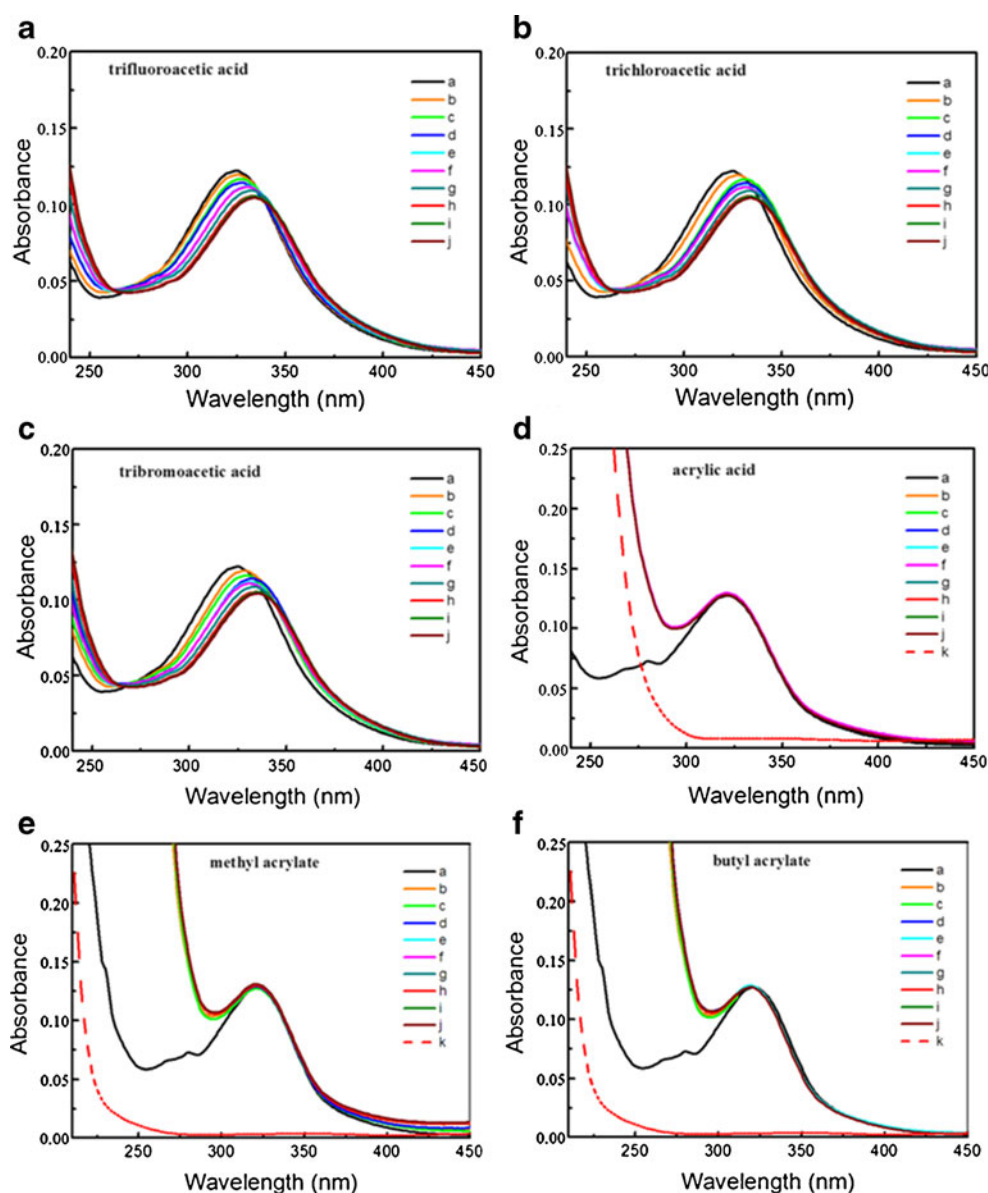
and the interaction of carboxylate ions and P9AF rings. From Fig. 5, we can see that the complexes of P9AF with AcO^- and benzoate through hydrogen bonding interactions are the most stable and hydrogen bonding is the primary intermolecular interactions. As shown in Scheme 1, the carbonyl oxygen atoms of carboxylate anions can interact with amino hydrogen atoms of P9AF to form hydrogen bonds in the HEPES buffer, which work as efficient bridges to mediate electron transfer between hydrogen-bonded species and initiate the so-called proton coupled electron transfer.

Possible Interaction Mechanism for Carboxylates and P9AF

Afore-mentioned results indicated that carboxylate anions could be recognized using P9AF in the HEPES buffer (pH

7.4), and substituent groups in carboxylate anions affected the interaction between $-\text{COO}^-$ and P9AF. To further explore the interaction between P9AF and carboxylate anions, we detected a variety of carboxylates using P9AF in the same conditions. As shown in Fig. 6a, the relative fluorescence quenching efficiencies of P9AF with carboxylic acids were in decreasing order: formic acid (a) \approx acetic acid (b) > propionic acid (c) > isobutyric acid (d) > benzoic acid (f) > pivalic acid (e) > acrylic acid (k) > 9-fluorencarboxylic acid (g). This suggested that these carboxylic acids could be sensed by P9AF, and the interaction decreased with the increasing of substituent groups in the side chain, which was due to the steric effect of substituent groups. Take acrylic acid for example, the calculation results revealed that hydrogen-bonding interactions were the primary intermolecular interactions (Fig. 7a). Moreover, the relative fluorescence quenching efficiencies of P9AF with

Fig. 8 UV-vis titration of P9AF in the HEPES buffer (pH 7.4) with increasing concentration of carboxylates: a blank; b 9.99×10^{-8} M; c 4.99×10^{-7} M; d 9.97×10^{-7} M; e 4.98×10^{-6} M; f 9.95×10^{-6} M; g 4.97×10^{-5} M; h 9.93×10^{-5} M; i 4.96×10^{-4} M; j 9.91×10^{-4} M

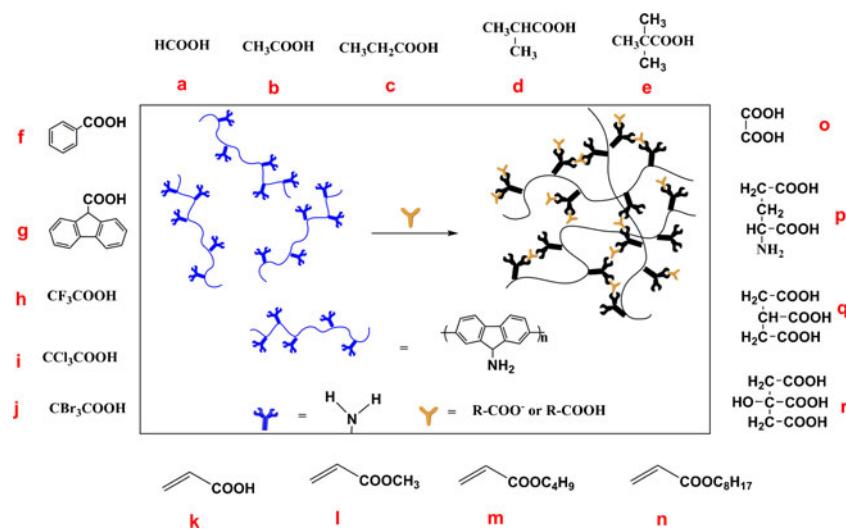


halogenated carboxylic acids were in decreasing order: acetic acid (b) > trifluoroacetic acid (h) > trichloroacetic acid (i) > tribromoacetic acid (j) (Fig. 6b). The interaction slightly decreased with the increasing of radiuses of halogen atoms, which further confirmed steric hindrance could affect the formation of hydrogen bonds between carbonyl oxygen atom of carboxylates and amino hydrogen atom of P9AF. Similar to acrylic acid, our DFT calculations proved that hydrogen-bonding interactions were the primary intermolecular interactions for the complex of P9AF and trifluoroacetic acid (Fig. 7b). To our surprise, acrylic esters hardly quenched the intensity, and acrylic acid quenched a small intensity of P9AF (Fig. 6c). This was due to alkyl groups in esters hindering acrylic esters near P9AF and then decreased the formation of hydrogen bonds between P9AF and acrylic esters. Additionally, carboxylic esters could not dissociate into carboxylate anions and hydrogen-bonds hardly formed between carboxylic esters and P9AF. Considering solvent effects, we also did the same experiment following the procedure in Fig. 6c, just using the series solution (ethanol) without acrylic esters. The fluorescence gram was shown in Fig. S4 and the addition of ethanol with different volumes caused almost no quench. From recognition carboxylates using P9AF, it could be see the relative fluorescence quenching efficiencies decreased with introduction of substituent groups, but they slightly increased with increasing the number of –COOH in the low concentration of carboxylic acids. Then, we detected some other carboxylic acids which have different number of –COOH and different substituent groups. In the low concentration of carboxylic acids, the relative fluorescence quenching efficiencies of P9AF with these carboxylic acids were in increasing order: acetic acid (b) < glutamic acid (p) < oxalic acid (o) < citric acid (r) ≤ tricarballic acid (q) (Fig. 6d). The relative fluorescence quenching efficiencies obviously increased with the increasing number of –COOH (from b, o, q), which could be beneficial to enhance the interaction between

carboxylates and P9AF due to the increasing number of hydrogen bonds. However, there was almost no fluorescence quenching increase of tricarballic acid (q) in comparison to citric acid (r) and obviously fluorescence quenching increase of oxalic acid (o) compared with glutamic acid (p). This was possibly due to the formation of intramolecular hydrogen bonds between substituent groups (–NH₂ or –OH) and –COOH/–COO[–], which influenced the formation of intermolecular hydrogen bonds. In addition, the fluorescence quenching efficiencies of P9AF were not influenced with increasing the number of –COOH in the high concentration of carboxylic acids, indicating the analyte-receptor saturation. Absorption spectra of P9AF showed a redshift upon addition of trifluoroacetic acid, trichloroacetic acid, and tribromoacetic acid which accorded with AcO[–] (Fig. 8). However, the absorption spectra of P9AF did not change at 325 nm upon addition acrylic acid/acrylates. It showed that the interaction between acrylic acid/acrylates and P9AF was weak compared with AcO[–].

These tested carboxylic acids easily dissociate into carboxylate anions in the HEPES buffer (pH 7.4). But no matter what forms carboxylates exist (excluding carboxylic esters), it is successful to detect carboxylates using P9AF via fluorescence quenching and hydrogen-bonding interactions are the primary molecular interactions. This indicates that P9AF can be applied as a satisfactory carboxylate sensor in this system. However, carboxylic esters can be hardly detected by P9AF via fluorescence quenching, which is mainly because carboxylic esters cannot dissociate into carboxylate anions, and hydrogen bonds can hardly form between carboxylic esters and P9AF. The possible sensing mechanism of P9AF is shown in Scheme 2. Since one carboxylate can coordinate with one or more 9AF units in the different polymer chains via hydrogen bonds, the coordination may cause the perturbation of the HOMO energy levels of the sensors mainly localized on the fluorene

Scheme 2 Schematic illustration of the sensing mechanism of P9AF for carboxylates



moieties and lead to the aggregation of polymer chains. A red shift in the absorption shows the presence of the anion raises the energy level of the HOMO. It is well-known that polymer chain can form a coil in solution depending on the surrounding environment and hydrogen bonds can enhance this aggregation, which leads to a significant quenching of P9AF emission.

Conclusions

In conclusion, water-soluble fluorescent P9AF has been successfully synthesized via electrochemical polymerization and was used as an efficient and practical technique for the detection of AcO^- in the HEPES buffer (pH 7.4). Additionally, this sensor was employed to recognize a variety of carboxylates and a possible mechanism was proposed. UV-vis spectra and DFT calculations indicated that the binding interactions between P9AF and carboxylates were described as intermolecular hydrogen bonds. This investigation provides new opportunities and fundamental guidelines for designing CP-based chemo/biosensor. The proposed chemosensor can pave the way for further practical use in biological science and plant physiology.

Acknowledgements The authors thank NSFC (51073074, 51272096), Jiangxi Provincial Department of Education (GJJ11590, GJJ10678) and Natural Science Foundation of Jiangxi Province (2010GZH0041) for providing financial support for this study.

References

- Martínez-Máñez R, Sancenón F (2003) Fluorogenic and chromogenic chemosensors and reagents for anions. *Chem Rev* 103:4419–4476
- Suksai C, Tuntulani T (2003) Chromogenic anion sensors. *Chem Soc Rev* 32:192–202
- Caltagirone C, Gale PA (2009) Anion receptor chemistry: highlights from 2007. *Chem Soc Rev* 38:520–563
- Moragues ME, Martínez-Máñez R, Sancenón F (2011) Chromogenic and fluorogenic chemosensors and reagents for anions. A comprehensive review of the year 2009. *Chem Soc Rev* 40:2593–2643
- Gale PA (2010) Anion receptor chemistry: highlights from 2008 and 2009. *Chem Soc Rev* 39:3746–3771
- Fabbrizzi L, Poggi A (2013) Anion recognition by coordinative interactions: metal-amine complexes as receptors. *Chem Soc Rev* 42:1681–1699
- Wenzel M, Hiscock JR, Gale PA (2012) Anion receptor chemistry: highlights from 2010. *Chem Soc Rev* 41:480–520
- Nguyen TQ, Wu JJ, Doan V, Schwartz BJ, Tolbert SH (2000) Control of energy transfer in oriented conjugated polymer-mesoporous silica composites. *Science* 288:652–656
- Thomas SW, Joly DG, Swager TM (2007) Chemical sensors based on amplifying fluorescent conjugated polymers. *Chem Rev* 107:1339–1386
- Swager TM (1998) The molecular wire approach to sensory signal amplification. *Acc Chem Res* 31:201–207
- McQuade DT, Pullen AE, Swager TM (2000) Conjugated polymer-based chemical sensors. *Chem Rev* 100:2537–2574
- Harrison BS, Ramey MB, Reynolds JR, Schanze KS (2000) Amplified fluorescence quenching in a poly(p-phenylene)-based cationic polyelectrolyte. *J Am Chem Soc* 122:8561–8562
- Yang JS, Swager TM (1998) Fluorescent porous polymer films as TNT chemosensors: electronic and structural effects. *J Am Chem Soc* 120:11864–11873
- Fan C, Plaxco KW, Heeger AJ (2002) High-efficiency fluorescence quenching of conjugated polymers by proteins. *J Am Chem Soc* 124:5642–5643
- McCullough RD, Ewbank PC, Loewe RS (1997) Self-assembly and disassembly of regioregular, water soluble polythiophenes: chemoselective ionchromatic sensing in water. *J Am Chem Soc* 119:633–634
- Gaylord BS, Heeger AJ, Bazan GC (2003) DNA hybridization detection with water-soluble conjugated polymers and chromophore-labeled single-stranded DNA. *J Am Chem Soc* 125:896–900
- Kim J, McQuade DT, McHugh SK, Swager TM (2000) Ion-specific aggregation in conjugated polymers: highly sensitive and selective fluorescent ion chemosensors. *Angew Chem* 112:4026–4030
- Kimura M, Horai T, Hanabusa K, Shirai H (1998) Fluorescence chemosensor for metal ions using conjugated polymers. *Adv Mater* 10:459–462
- Chen L, McBranch DW, Wang HL, Helgeson R, Wudl F, Whitten DG (1999) Highly sensitive biological and chemical sensors based on reversible fluorescence quenching in a conjugated polymer. *P Natl Acad Sci USA* 96:12287–12292
- Li C, Numata M, Takeuchi M, Shinkai S (2005) A sensitive colorimetric and fluorescent probe based on a polythiophene derivative for the detection of ATP. *Angew Chem* 44:6371–6374
- Fan CH, Wang S, Hong JW, Bazan GC, Plaxco KW, Heeger AJ (2003) Beyond superquenching: hyper-efficient energy transfer from conjugated polymers to gold nanoparticles. *P Natl Acad Sci USA* 100:6297–6301
- Zhu CL, Liu LB, Yang Q, Lv FT, Wang S (2012) Water-soluble conjugated polymers for imaging, diagnosis, and therapy. *Chem Rev* 112:4687–4735
- Groenendaal LB, Gianni Z, Auber PH, Waybright SM, Reynolds JR (2003) Electrochemistry of poly(3,4-alkylenedioxythiophene) derivatives. *Adv Mater* 15:855–879
- Gao YW, Bai H, Shi GQ (2010) Electrosynthesis of oligo(methoxyl pyrene) for turn-on fluorescence detection of volatile aromatic compounds. *J Mater Chem* 20:2993–2998
- Chen YQ, Bai H, Hong WJ, Shi GQ (2009) Fluorescence detection of mercury ions in aqueous media with the complex of a cationic oligopyrene derivative and oligothymine. *Analyst* 134:2081–2086
- Chen YQ, Shi GQ (2009) Fluorescence detection and discrimination of ss- and ds-DNA with a water soluble oligopyrene derivative. *Sensors* 9:4164–4177
- Chen YQ, Bai H, Chen Q, Li C, Shi GQ (2009) A water-soluble cationic oligopyrene derivative: spectroscopic studies and sensing applications. *Sens Actuators B Chem* 138:563–571
- Grell M, Bradley DDC, Inbasekaran M, Woo EP (1997) A glass-forming conjugated main-chain liquid crystal polymer for polarized electroluminescence applications. *Adv Mater* 9:798–802
- Lu HH, Liu CHY, Chang CHH, Chen SA (2007) Self-dopant formation in poly(9,9-di-n-octylfluorene) via a dipping method for efficient and stable pure-blue electroluminescence. *Adv Mater* 19:2574–2579
- Huang F, Niu YH, Zhang Y (2007) A conjugated, neutral surfactant as electron-injection material for high-efficiency polymer light-emitting diodes. *Adv Mater* 19:2010–2014
- Kim HN, Guo ZQ, Zhu WH, Yoon JY, Tian H (2011) Recent progress on polymer-based fluorescent and colorimetric chemosensors. *Chem Soc Rev* 40:79–93
- Pu KY, Liu B (2009) Conjugated polyelectrolytes as light-up macromolecular probes for heparin sensing. *Adv Funct Mater* 19:277–284

33. Fan CL, Xu JK, Chen W, Dong B (2008) Electrosynthesis and characterization of water-soluble poly(9-aminofluorene) with good fluorescence properties. *J Phys Chem C* 112:12012–12017
34. Fan CL, Xu JK, Chen W, Lu BY, Miao HM, Liu CC, Liu GD (2009) Polyfluorene derivatives with hydroxyl and carboxyl substitution: electrosynthesis and characterization. *J Phys Chem C* 113:9900–9910
35. Lu BY, Xu JK, Fan CL, Miao HM, Shen L (2009) Electrochemical polymerization of benzantrone and characterization of its excellent green-light-emitting polymer. *J Phys Chem B* 113:37–48
36. Zhang G, Lu BY, Wen YP, Lu LM, Xu JK (2012) Facile fabrication of a cost-effective, water-soluble, and electrosynthesized poly(9-aminofluorene) fluorescent sensor for the selective and sensitive detection of Fe(III) and inorganic phosphates. *Sens Actuators B Chem* 171–172:786–794
37. Frisch MJ, Trucks GW, Schlegel HB, Scuseria GE, Robb MA, Cheeseman JR, Scalmani G, Barone V, Mennucci B, Petersson GA et al (2009) Gaussian 09, revision A.02. Gaussian, Inc, Wallingford
38. Yardim Y, Erez ME (2011) Electrochemical behavior and electroanalytical determination of indole-3-acetic acid phytohormone on a boron-doped diamond electrode. *Electroanal* 23:667–673
39. Gunnlaugsson T, Davis AP, Hussey GM, Tierney J, Glynn M (2004) Design, synthesis and photophysical studies of simple fluorescent anion PET sensors using charge neutral thiourea receptors. *Org Biomol Chem* 2:1856–1863
40. Lee SK, Kim H, Jang S, Kang J (2011) Carboxylate selective anion receptor based on two anthracenes with malonamide spacer. *Tetrahedron Lett* 52:1977–1980
41. Zhang X, Guo L, Wu FY, Jiang YB (2003) Development of fluorescent sensing of anions under excited-state intermolecular proton transfer signaling mechanism. *Org Lett* 5:2667–2670
42. Wu FY, Li Z, Wen ZC, Zhou N, Zhao YF, Jiang YB (2002) A novel thiourea-based dual fluorescent anion receptor with a rigid hydrazine spacer. *Org Lett* 4:3203–3205
43. Goswami S, Das AK, Sen D, Aich K, Fun HK, Quah CK (2012) A simple naphthalene-based colorimetric sensor selective for acetate. *Tetrahedron Lett* 53:4819–4823
44. Hosseini M, Ganjali MR, Veismohammadi B, Faridbod F, Abkenar SD, Salavati-Niasari M (2012) Selective recognition of acetate ion based on fluorescence enhancement chemosensor. *Luminescence* 27:341–345
45. Sathish S, Narayan G, Rao N, Janardhana C (2007) A self-organized ensemble of fluorescent 3-hydroxyflavone-Al (III) complex as sensor for fluoride and acetate ions. *J Fluoresc* 17:1–5
46. Huang WW, Lin H, Lin HK (2011) Fluorescent acetate-sensing in aqueous solution. *Sens Actuators B Chem* 153:404–408